Research Article – Vol. 02, Issue 02, No. 06

Advanced in Engineering and Intelligence Systems

Journal Web Page: https://aeis.bilijipub.com

Simulation, optimization and thermodynamic, economic and environmental analysis of cryogenic cycle, dew point regulation in an existing refinery

Ehsanolah Assareh [a, *], Mojtaba Nedaei [b,c], Sajjad keykhah [d]

[1] *School of Chemical Engineering, Yeungnam University, Gyeongsan 38541, South Korea**
[2] *Department of Management and Engineering, University of Padua (Padova), Vicenza, Italy*
[3] *University of Warsaw, Warsaw, Poland*
[4] *Department of Mechanical Engineering, Dezful Branch, Islamic Azad University, Dezful, Iran*

Highlights

- Proposal of an optimal structure for improved performance of the dew point adjustment unit.
- Simulation of current and optimal processes using ASPEN HYSYS software.
- Sensitivity analysis of turbo-expander outlet pressure effects.
- Utilizing waste gas temperature to condense vapors in the Optimal design.
- Indicating increased exergy efficiency, reduced carbon footprint, and 11.54% savings in NGL value production costs.

Article Info

Received: 15 April 2023
Received in revised: 28 May 2023
Accepted: 28 May 2023
Available online: 29 June 2023

Keywords

Exergy analysis,
environment,
footprint,
energy,
simulation

Abstract

Energy is one of the critical parameters for sustainable development in any nation. Technology progress and lifestyle change have led to increased energy demand. In this paper, an optimal structure for thermodynamic, environmental and economic improvement of the existing dew point adjustment unit (South Pars Energy Zone in Iran) is presented. Also, the analysis of the sensitivity of the turbo-expander outlet pressure on the total exergy efficiency, duty reboiler of gas-liquid distillation towers and the intensity of NGL product production in the current and optimal state has been performed. The current and optimal process is simulated by using Aspen Hysys software. The optimal structure used the low temperature of the waste gas to condense the vapors above the propane and butane towers, and by removing the air conditioners leads to energy recovery, increase in overall exergy efficiency and reduce in carbon dioxide emissions and NGL production costs. The optimization scenario showed that the total exergy efficiency increased to 0.7305 and the total exergy loss decreased by 23.22%. In the environmental sector, the optimal process resulted in a 39% reduction in carbon dioxide footprint, and economically, with annual savings of 3107549.45 $ in energy supply costs, it resulted in 11.54T reduction in NGL value production costs.

Nomenclature

Indices		***Variables***	
A	*Area (m2)*	*Greek Symbols*	
e_SIM	*Absolute average difference (%)*	*H*	*efficiency*
$\dot{E}$	*Exergy rate (kW)*	*Subscripts and superscripts*	
$\dot{E}_D$	*Destruction exergy rate (kW)*	*o*	*Dead state*
EDI	*Exergy destruction intensity (%)*	*A*	*Available*
h	*Specific enthalpy (kJ)*	*Ex*	*Exergy*
$\dot{m}$	*Flow rate (kg/h)*	*In*	*inlet*

*Corresponding Author: Ehsanolah Assareh
Email: Ehsanolah.assareh@gmail.com

MF	*Material factor (-)*	*Out*	*Outlet*
P	*Pressure (Pa)*	*P*	*Pump*
PF	*Pressure factor (-)*	*Ph*	*Physical*
$\dot{Q}$	*Heat transfer rate (kW)*	*Heat transfer rate (kW)*	*Ch*
RF	*Relative factor (-)*	*T*	*Turbine*
s	*Specific entropy (kJ/K)*	*Tot*	*Total*
T	*Temperature (K)*	*V*	*vapor*
$\dot{W}$	*Work or power (kW)*	*En*	*Energy*
V	*Volume (m3)*	*K*	*Component k*
TCI	*Total capital investment ($)*	*Abbreviations*	
TCI	*Total cost investment ($)*	*NGL*	*Natural gas liquid*

1. Introduction

The use of fossil fuels leads to a serious air pollution, and the emission of CO2 exhaust plays an important role in worldwide energy system [1]. In recent years due to the limitation of crude oil and its environmental effects, a replacement of natural gas as a cleaner source has become more important [2]. Nowadays cleaner fuels are needed and an alternative to crude oil has become a priority in the world. Natural Gas as a potential energy source which is widely used with high calorific value and low emission problems, so demanding for a much cleaner and safer alternative is highly required. Liquefied natural gas (LNG) is known as a source of clean energy which is commonly used as an industrial and domestic fuel for combustion. The only practical way for mass transportation of natural gas across oceans is LNG (liquefied natural gas). LNG is also the suitable to use for natural gas resources derived from remote gas fields, offshore gas, methane, and other unconventional gas sources. Therefore, in recent years, LNG technology has developed rapidly. Due to its significant energy content, liquefied natural gas (LNG) including propane, ethane, methane and etc has different applications such as agricultural, commercial, industrial and household consumptions [3,4]. Efficient and new methods of energy production have become a central issue for researchers due to the rapid change of energy consumption rate in societies. Researchers in recent years have shown a growing interest in using waste heat sources, engines and waste heat from industrial plants and exhaust stream from gas turbine, as the high temperature sources of a bottoming cycle [5–9]. Natural gas liquid (NGL) separation is an important link in any LNG plant. Johnson et al. conducted the research in recent technical advances for high NGL recovery [10]. Due to the better appreciation of the refrigeration integration between LNG and NGL sections, expander-based process has received increased attention in recent years [11]. Jibril et al studied natural gases of different turbo expander process configurations in wide range compositions [12]. LNG is composed of 85–99% methane by mole fraction, and propane depending on where it is produced and a few percent ethane. Rising in the price of energy sources has caused cryogenic natural gas liquid recovery plants to be more efficient and complex. In other words, the new generation of NGL is created based on reducing the operating costs of the plant for a particular output. New design projects are going to find ways to minimize the cost of on new capital and maximize the use of existing equipment [13,14]. Accordingly, the use of LNG cold energy is an interesting field of study. The potential of cold energy includes air liquefaction power generation, separation and refrigeration, cryogenic thermoelectric generator, reduction of CO2 emission, and similar applications to cold usage [15–19]. Propane and ethane or a mixture of both as refrigerant could be used in some systems. Refrigeration is also provided by work expansion of the compressed natural gas or turbo- expander. Separation of propane ,Ethane, Methane and natural gas liquids (NGL) is generally carried out in a refinery plant [20,21].Several NGL process configurations have been investigated to increase the process efficiency and decrease the operating costs [22–24]. Ghorbani et al. [25–27] have presented the results of the exergy analyses using the total revenue requirements (TRR) method in a gas separation process. Also, Ghorbani et al. have presented the results of the using absorption refrigeration cycle [28,29]. Other researchers presented the optimization of the NGL plant performance [30–32]. The process temperature in NGL recovery cycle may reach to −60 °C as the lowest. The required refrigeration is achieved by propane refrigeration cycles in such processes [33]. By adjusting the operating conditions the performance of NGL plants can be significantly improved. According to several research works [34,35].Vatani et al. [36] have introduced a new process configuration for production of LNG and NGL. They have considered all of the process limitations in the case of LNG liquefaction processes and NGL recovery. There are several studies [37–39] have introduced different cycles about LNG plants and NGL with compression refrigeration. The most important factor is the optimum operating condition which can significantly influence the plant efficiency. Nogal et al. [40] have presented a new approach for the optimal design. In addition, Alabdulkarem et al. [41] Investigated the performance enhancement of a propane pre-cooled mixed refrigerant LNG plant. Mehrpooya et al. [42] introduced a high efficiency of NGL process configuration. A large amount of energy to liquefy air is required for

Cryogenic distillation [43]. Sensible heat of vaporization of air can be exchanged with the condensation heat of pure nitrogen in the two-column separation process by combining the condenser of the high-pressure column with the reboiler of the low-pressure column [44,45]. Thus, the energy consumption of the process can be reduced by heat recovery [46e48]. Due to the electricity needed to compress the air feed, a large pressure difference is required between the high and low pressure columns so the energy cost for producing pure oxygen remains relatively high [49,50]. In the regasification process, the cold energy obtained in the liquefaction process has to be released before the final utilization of the industrial gas products because. Most of the time, these cryogenic liquids cannot be used directly.

In this paper, an optimal structure for thermodynamic, environmental and economic improvement of the existing dew point adjustment unit (South Pars Energy Zone in Iran) is presented. Also, the analysis of the sensitivity of the turbo-expander outlet pressure on the total exergy efficiency, duty reboiler of gas-liquid distillation towers and the intensity of NGL product production in the current and optimal state has been performed.

2. Description of the case study process

Figure (1) shows the flow diagram in the current process. The purpose of this process is to cool natural gas using a turbo-expander and to produce gaseous liquids and then to separate the gaseous liquids in the distillation towers. The main products of this unit are waste gas, propane, butane and pentane plus condensate. The natural gas flow is partially cooled by passing through the E-101 to E-103 heat exchangers, and in the D-101 separator at this stage the primary gaseous liquids are separated. Then, the upper steam of the separator is expanded by the GX-101 expansion turbine and the work resulting from this expansion is provided to the K-101 compressor to send the waste gas as a compact reinforcement to the compression and cooling unit for final compression [51].

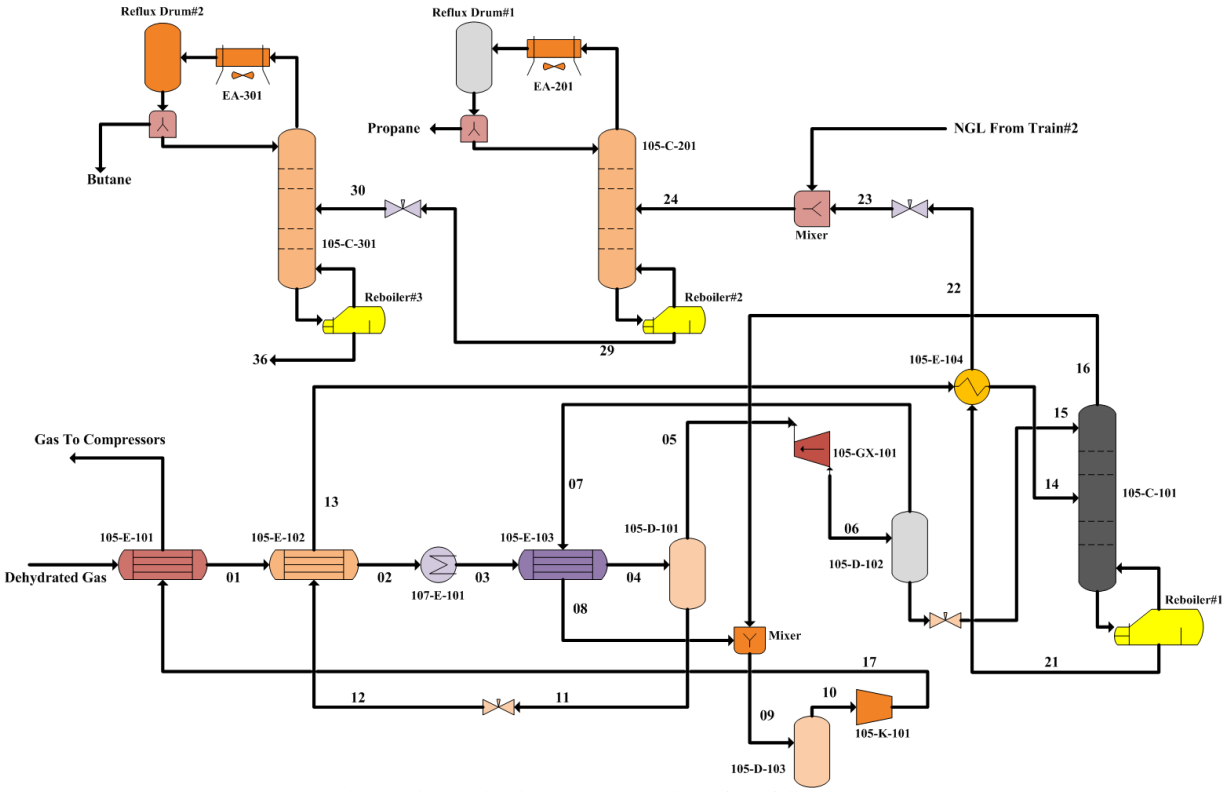

Fig. 1. The production process consists of the following parts

The outlet fluid from the expander enters the D-102 separator in two phases at low temperature to separate the gaseous liquids again. The cold vapors above this separator are used in the E-103 heat exchanger to cool natural gas and then enter the k-101 compressor [1]. In order to separate the possible liquids before the K-101 compressor, the D-103 separator was used in order to prevent the liquid from entering the compressor. Separated liquids from separators D-101 and D-102 enter the de-ethanizer distillation tower by passing through Jules Thomson valves to separate ethane and methane. The de-ethanizer tower is fed in such a way that the flow of hydrocarbon liquid obtained from the D-102 separator enters from the highest tray because it has a lower temperature, and the gaseous liquids produced

from D-101 separator enter from the middle of the C-101 tower. The cold steam at the top of the C-101 de-ethanizer tower, along with the waste gas above the D-102 separator, enters the K-101 compressor and forms the waste gas product [1]. This gas stream is sent to the compression unit at a higher temperature by passing through the E-101 heat exchanger. The liquid produced from the C-101 de-ethanizer tower reboiler, by passing through the E-104 heat exchanger, increased the temperature of the gaseous liquids to some extent and was sent to the propane and butane distillation unit with a lower temperature. It should be noted that the gaseous liquids taken from the part 2 are also mixed with the part 1 and enter the C-201 propane distillation tower. In the depropnazier tower, the propane product comes out of the butane plus reboiler and enters the debuthanizer tower. Finally, the butanes are separated from pentane plus by a debuthanizer distillation column and produced from a condenser and a reboiler, respectively. Table (1) provides information on de-ethanizer, depropnazier and debuthanizer distillation towers.

Table 1. Information and specifications of distillation towers [51]

Subject	De-ethanizer tower	Depropnazier tower	Debuthanizer tower
Number of trays	44	46	34
Feed tray	24	28	14
High pressure	-3101	2201	751/3
Low pressure	3141	2241	791/3
Condensing temperature	-	59/3	58
Reboiler temperature	115/6	134	97

Table 2. Information and specifications of current process flows [51]

Stream	T (°C)	P (kPa)	F($\frac{kmole}{h}$)	stream	T (°C)	P (kPa)	F($\frac{kmole}{h}$)
Dehydrated Gas	25.9	7231	31660	01	13.6	7201	31660
03	-13.2	7091	31660	02	9.5	7141	31660
04	-31.8	7041	31660	05	-31.8	7041	30590
06	-66	3301	30590	07	-66.4	3301	28500
15	-67.9	3101	2087	13	5.8	3301	1074
10	-33	3101	30800	17	-7.4	4152	30800
09	-32.8	3101	30800	08	-35.13	3171	28500
16	-23.5	3101	2299	21	115.6	3141	861.2
22	54.6	2991	861.2	23	40.5	2221	861.2
24	40.4	2181	1729	propane	59.3	2201	764.3
29	134	2241	965	30	85.6	771.3	965
Butane	58	751.3	405.4	36	96.1	791.3	559.6

3. Feed gas specification

Figure (2) shows the operational units for processing raw natural gas and delivering it to the gas-liquid distillation unit in phase 6 of the South Pars Gas Complex Company (Iran). The raw gas stream is first refined in the sweetening unit using an alkanolamine solvent and loses its acid gases.

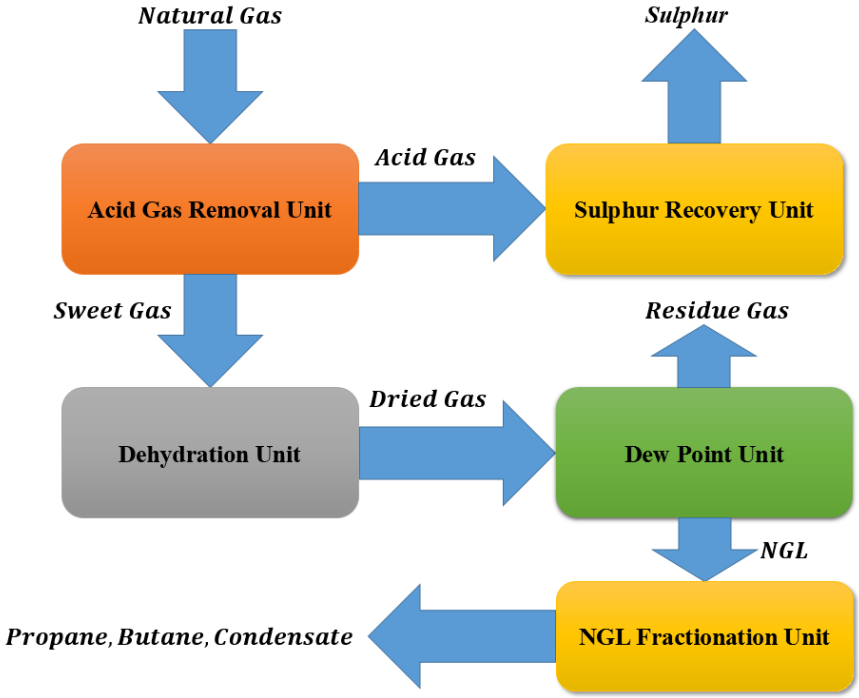

Fig. 2. Chart of natural gas processing in phase 6 of South Pars gas complex

Acid gases are converted to elemental sulfur in another unit called sulfur recovery, and the sweetened gas enters the dehumidification unit, where water is removed from the sweetened natural gas using solid media (molecular sieve) .This will prevent frostbite in downstream processes. The dried gas, which is the main product of the dehydration unit, is the feed of the dew point regulation unit, the composition of which is presented in table (3). In the dew point adjustment unit, based on turbo expansion, the temperature of natural gas decreases and valuable hydrocarbons such as ethane, propane to condensate are separated from natural gas. This liquid stream is known as natural gas liquids and it is necessary to separate and produce these hydrocarbons in another unit called NGL distillation.

Table 3. Feed composition of dew point adjustment unit [51]

Combination	Component Molar	Combination	Component Molar
Methane	0.8561	p-Xylene	0.0001
Ethane	0.0541	n-Nonane	0.0001
Propane	0.0180	Cumene	0.0000
i-Butane	0.0041	n-Decane	0.0000
n-Butane	0.0063	n-C11	0.0000
i-Pentane	0.0018	Nitrogen	0.0311
n-Pentane	0.0015	CO_2	0.0184
Mcyclopentan	0.0001	H_2S	0.0062
Benzene	0.0001	H_2O	0.0000
n-Hexane	0.0009	Methyl-Mercaptan	0.0000
Cyclohexane	0.0001	Ethyl-Mercaptan	0.0001
Mcyclohexane	0.0001	COS	0.0000
Toluene	0.0000	Propyl Mercaptan	0.0000
n-Heptane	0.0005	Butyl Mercaptan	0.0000
n-Octane	0.0002	1Pentanthiol	0.0000

4. Simulation properties package

The computational core of the process is in the simulation of the thermodynamic equation. In aspen Hysys software version 10, thermodynamic equations have the following types [52]:

1- Steam equations like ASME Steam

2- State equations such as SRK and Peng Robinson

3- Various equations such as Acid Gas-Chemical Solvents

4- Activity equations such as UNIQUAC and NRTL

In this simulation work, the equations of state and Peng Robinson equation are used. Choosing the right equation has a great effect on the accuracy of the simulation and increases the validity of the results obtained from the simulation, so choosing the right equation is very important. The Peng Robinson equation is widely used to simulate natural gas processes, aromatics production, and air separation. For the process of operations at high pressure, high temperature and with non-ideal gas phase to calculate the thermodynamic properties, the Peng Robinson state equation should be used, the formulation of which is described in Equation (1) [53].

$$P = \frac{RT}{V_m - b} - \frac{a \propto}{V_m(V_m - b)} \quad (1)$$

The compressibility factor Z and the fugacity coefficient φ for compound i in a mixture are shown as Equations (2) and (3) [53]:

$$Z^3 - (1 - B)Z^2 + (A - 3B^2 - 2B)Z - (AB - B^2 - B^3) = 0 \quad (2)$$

$$\ln\emptyset_i = \frac{b_i}{B}(Z - 1) - \ln(Z - B) - \frac{A}{2\sqrt{2B}}\left(\frac{b_i}{B} - \frac{2}{a\alpha}\sum_j y_i(a \propto_{ij})\right)\ln\frac{Z + (1 + \sqrt{2})B}{Z + (1 - \sqrt{2})B} \quad (3)$$

The Peng Robinson equation is ideal for calculating liquid-vapor equilibrium plus fluid densities for hydrocarbon systems. Several improvements have been made to the early Peng Robinson model to extend its scope of application, and its predictions have been made for some unusual systems. However, in situations where the system is not ideal, the use of activity models is recommended. The Peng Robinson feature package solves any three-, two-stage, or single-stage system with a high degree of efficiency and reliability and is applicable to a wide range of applications [53]. The Peng Robinson equation also includes improved binary interaction parameters for all total hydrocarbon-hydrocarbon pairs, as well as for hydrocarbon-non-hydrocarbon binaries. For hydrocarbon or non-group components, hydrocarbon-hydrocarbon interaction parameters are automatically generated by Hysys for predictions of improved liquid-vapor balance properties. For oil, gas, and petrochemical tools, the Peng-Robinson equation of state is a general feature package [53].

5. Simulation

In this paper, Aspen Hysys software is used to simulate the current process and the optimal state. The schematic of the simulation is shown in Figure (3). Heat exchangers used to coling natural gas are modeled as shell-tubes and used in flowsheet. Also, to simulate the distillation towers and separation of gaseous liquids, Rigorous model columns have been used, which have high accuracy. Also, the spreadsheet tool has been used to perform exergy and environmental calculations.

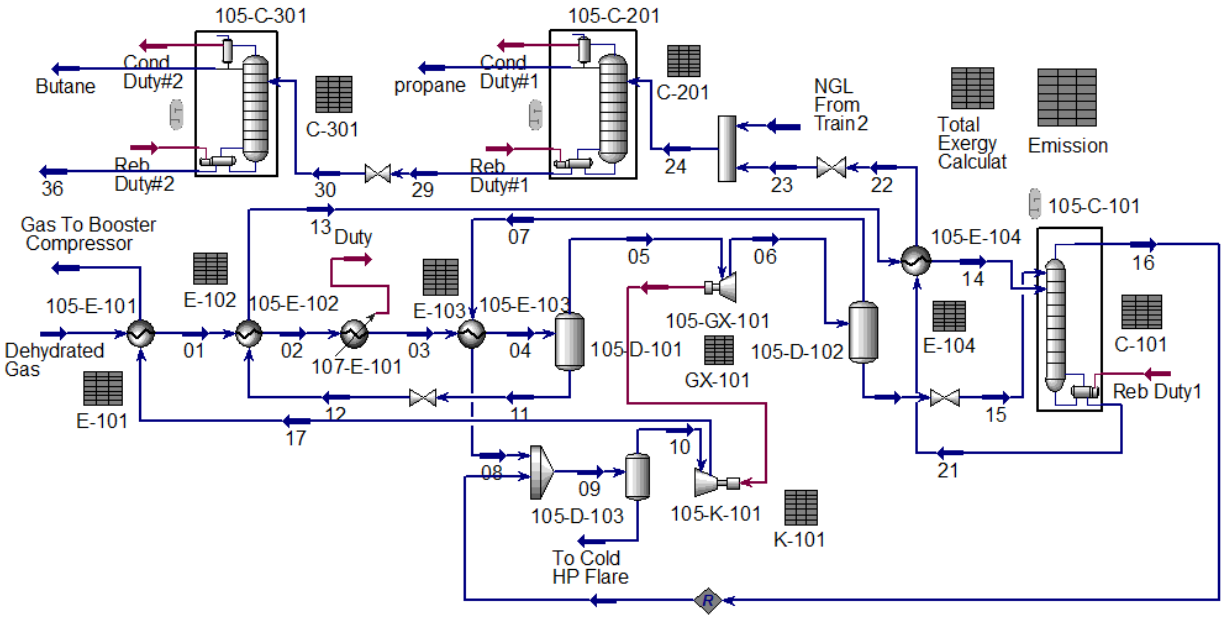

Fig. 3. Schematic of current trend simulation (without optimization)

6. Simulation validation

The design of gas refineries requires very repetitive calculations. In the past, design calculations were done entirely manually, with diagrams and thermodynamic tables and other features being very important tools. Among these complex calculations, the most important properties required to perform basic calculations based on a state equation are obtained. These properties include molar volume, enthalpy, Gibbs free energy, and fugacity coefficients for all materials in the process. As mentioned in this paper, Aspen Hysys software is used to simulate and Peng Robinson equation for property calculations (Figure 3). On the other hand, in order to improve the thermodynamic, environmental and economic current trends, a new design based on thermal integration has been proposed; therefore, it is necessary to determine the accuracy and validity of the simulation results of the current process. Equation (4) [54] measures the value of the AARD parameter for each test and all tests performed.

$$\emptyset_{AARD}[\%] = \frac{1}{m}\left(\sum_{i}^{m}\left|\frac{x_i^{op} - x_i^{cal}}{x_i^{op}}\right|\right) \times 100 \qquad (4)$$

Where x_i^{op} and x_i^{cal} are the actual data calculated by the software, respectively, and m is the number of comparison points. In this regard, after simulating the current trend and obtaining the results from the software, these results are compared with existing industrial data, which is reported in Table (4). According to Table (4), the temperature results from the Peng Robinson equation equations are very well matched with the available industrial data, so that the error rate obtained according to Equation (4) is equal to 2.12%. The value of the calculation error indicates that the selected state equation is very suitable and is also recommended for simulating similar units.

Table 4. Compare results at key points in the process

Subject	X_{plant} [1]	X_{sim}	$\left\|\frac{X_{plant} - X_{sim}}{X_{plant}}\right\|$
High tempretature of de-ethanizer (℃)	0-23/5	23/62	0/0051
Reboiler temperature of de-ethanizer (℃)	115/60	115/60	0
High tempretature of depropnazier (℃)	59/3	59/05	0/00421
Reboiler temperature of depropnazier (℃)	134	136/2	0/0015
High tempretature of debuthanizer (℃)	58	58/66	0/0113
Reboiler temperature of debuthanizer (℃)	96/1	97/01	0/0095
Expander outlet temperature(℃)	-67/74	-660	0/004
Feed temperature of de-ethanizer tower(℃)	-67/9	-67/28	0/00913
Feed temperature of depropnazier tower(℃)	40/5	46/04	0/136

Feed temperature of debuthanizer tower(℃) Error	85/6 0/0212	88/45	0/0322

7. Optimization structure

Thermal integration is a method to minimize energy consumption based on thermodynamic equations. This goal is achieved by optimizing heat recovery systems, process energy supply methods and operating conditions. This technology is also known as thermal integration, energy integration. Figure (4) shows the process flow diagram for the optimization structure presented in this paper. This technology can be done in some refineries and can be implemented by implementing an efficient management of energy and various sources of supply in the process, to minimize investment costs and by saving this cost and obtain the economic benefits in the short term.

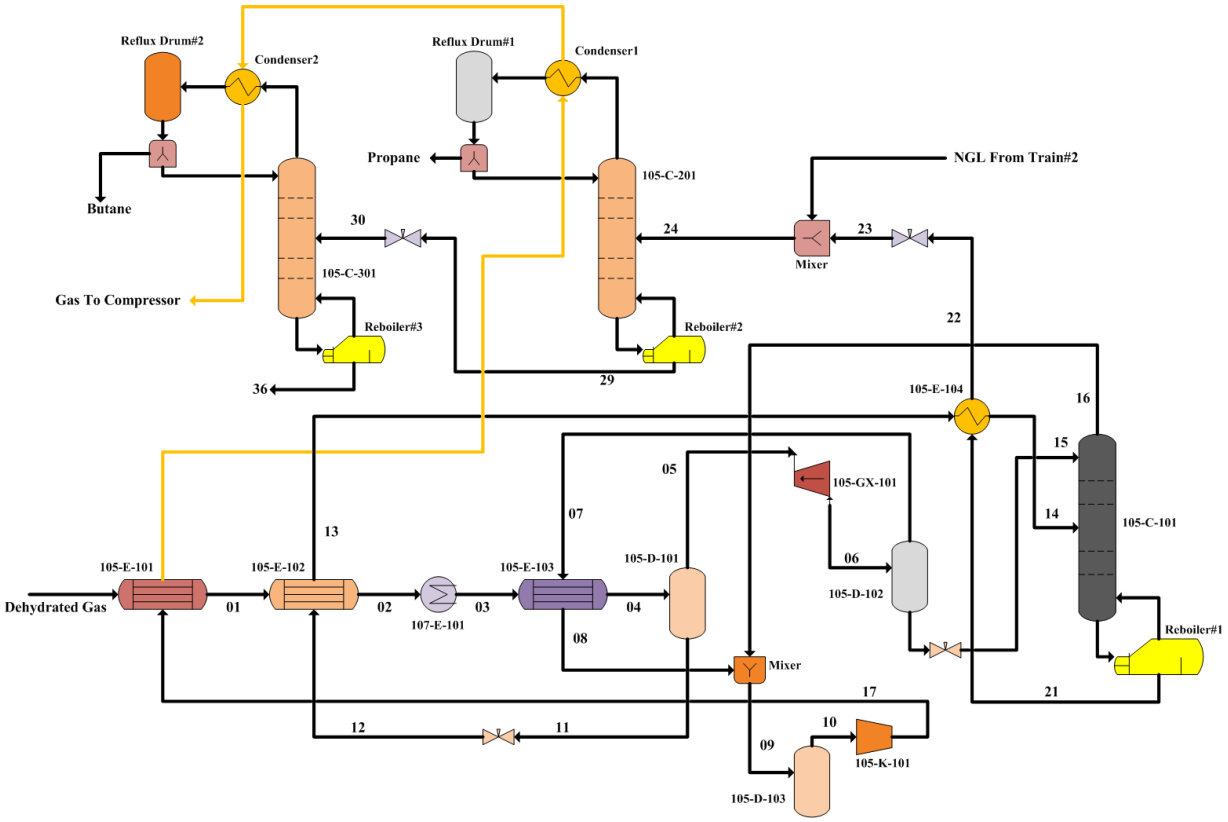

Fig. 4. Schematic of optimal structure process flow (proposed design)

This structure is based on thermal integration and operates in such a way that it removes both EA -201 and EA -301 air conditioners. As shown in Figure (4), the waste gas stream coming out of the E-101 heat exchanger has a suitable temperature that can be used to condense the vapors above the distillation towers in such a way that air conditioners are not required. The condensation temperature of the vapors in the C-301and C-201 distillation towers is much lower than the temperature of the waste gas output from the E-101 heat exchanger, thus making it possible for full energy integration. By doing this, for which the simulation has been done, two air conditioners will be removed from the process and their electricity consumption will be saved. On the other hand, with the reduction of electricity consumption due to the reduction of utility consumption, carbon dioxide emissions are also reduced, the exact values of which are also presented in the evaluation section of the results. This will replace the EA-201 and EA-301 air-conditioners with two process-process heat exchangers, named Condenser1 and Condenser2 in Figure 4, respectively. These heat exchangers are much more cost-effective than air conditioners in terms of cost and price, which will result in an economically justifiable proposal that has been discussed in the economic evaluation.

8. Process analysis

8.1. Economic evaluation

Table (5) shows the key parameters (direct cost, indirect cost, fixed cost of investment and cost of investment) and the calculation formulations. Equipment price (PEC) is repeated in most cases and the calculation of some of these parameters depends on the price of equipment. The price of equipment and the cost of installing equipment (Purchased-Equipment installation) have been calculated through the APEA section of Aspen Hysys software.The purpose of determining the parameters in Table (5) is to calculate the TCI value. By calculating the TCI value, the competitive and key parameter of the total annual cost (TAC) can be calculated and finally the total cost per kilogram of liquefied petroleum gas (CON) can be determined. The total annual cost depends on two TCI parameters and the total energy operating cost (Equation 5). Here the return on investment is assumed to be 3 years [55].

$$\mathrm{TAC} = \frac{\mathrm{TCI}}{\mathrm{payback}} + \text{Energy Cost} \tag{5}$$

The total cost of energy is also calculated by the APEA tool. After calculating the TCI and determining the amount of NGL produced, the amount of cost that must be incurred to produce each kilogram of NGL (Cost of NGL) is obtained through Equation (6). It is worth mentioning that the working year is equal to 8150 hours [57] (340 days).

$$\mathrm{CON}\left(\frac{\$}{\mathrm{kg_{NGL}}}\right) = \frac{\mathrm{TAC}}{\dot{m}_{\mathrm{NGL}}} \tag{6}$$

Table 5. Key parameters for economic estimation [6]

I.Fixed-Capital Investment (FCI)	
A. Direct Costs (DC)	
A.1. Onsite Costs (ONSC)	
Purchased-Equipment Cost (PEC)	PEC
Purchased-Equipment installation	90% PEC
Piping	70% PEC
Instrumentation and Controls	40% PEC
Electrical Equipment and materials	15% PEC
A.2. Offsite Costs (OFSC)	
Land	10% PEC
Civil, structural and architrctural work	90% PEC
Service facilities	100% PEC
Total direct costs (DC) = (ONSC) + (OFSC)	
B. Indirect Costs (IC)	
B.1. Engineering and supervision	75% PEC
B.2. Construction costs	15% DC
B.3. Contingencies	25% sum of above
Total indirect costs (IC)	
Total Fixed Capital Investment (FCI) = (DC) + (IC)	
II. Other Outlays	
Startup costs	12% FCI
Working capital	20% TCI
Allowance for funds used during construction	15% FCI
Total Capital Investment (TCI) = (FCI) + (Other Outlays)	

8.2. Environmental assessment

Overall carbon dioxide emission is a parameter that has been evaluated in this study. In the dew point adjustment unit, the compressor is powered by a natural gas expansion turbine, so there is no emission through it. However, the condensers of the distillation tower are depropnazier and debuthanizer type of air fan that uses electricity service. on the other hand, de-ethanizer, depropnazier and debuthanizer distillation towers reboilers, all provided with steam support

service; Therefore, in both cases, gas fuel should be used to supply electricity and steam, for which the refinery uses part of the produced gas as fuel.

The emission of carbon dioxide in a chemical process is usually in three different ways [57]:

1. Carbon dioxide does not react
2. Carbon dioxide emitted by providing steam utility
3. Carbon dioxide emitted through the electricity support service

The amount of carbon dioxide emitted can be calculated from Equation (7) [57]:

$$\text{Carbon Dioxide Emission}\left(\frac{\text{kg}}{\text{s}}\right) = \frac{\text{Q}_{\text{Req}}}{\text{LHV}} \times \frac{\%\text{C}}{100} \times 44 \qquad (7)$$

In the above relation, $\text{Q}_{\text{Req}}$is the amount of energy required (electricity or steam) in terms of $(\frac{\text{kj}}{\text{s}})$, LHV is the value of the fuel consumed in terms of $(\frac{\text{kj}}{\text{kg}})$ Also, the value of %C for natural gas is 75.4 and the number 44 indicates the molar mass of carbon dioxide [57].

It should be noted that in this study, due to the absence of a chemical reactor, the amount of unreacted carbon dioxide will be equal to zero. In addition, the calorific value of gaseous fuels for the production of utility reboilers and air conditioners is equal to $44540\frac{\text{kj}}{\text{kg}}$.

The competitive parameter presented here is the carbon dioxide footprint, which can be calculated and measured as Equation (8):

$$\text{CO}_2\ \text{Footprint}\left(\frac{\text{kg}_{\text{CO}_2}}{\text{kg}_{\text{NGL}}}\right) = \frac{\text{Carbon Dioxide Emission}}{\dot{\text{m}}_{\text{NGL}}} \qquad (8)$$

8.3. Thermodynamic evaluation

All thermodynamic processes are governed by the laws of conservation of mass and energy. These laws of survival state that mass and energy can neither be created nor destroyed in one process. However, the exergy does not remain, but is eliminated by the irreversibility of the system. As a result, an exergy balance must have a destructive expression that disappears only in a reversible process. In addition, exergy generally disappears when a stream of material or stream of energy is transferred to the environment. To perform exergy analysis, the amount of exergy and the amount of specific exergies must be calculated [58].Exergy loss is a measure of the thermodynamic efficiency of a process, and the lower the exergy loss, the higher the thermodynamic efficiency of the process and the lower the amount of energy is required. The maximum thermodynamic efficiency is achieved when the reversible process and the exergy loss are zero, which is practically not possible. Exergy loss in a distillation tower is obtained by balancing the exergy around the tower. Exergy loss in a tower is defined as the difference in input and output exergies [58].Exergy is a flow ($\dot{\text{E}}^{\text{i}}_{\text{Total}}$) the sum of physical ($\dot{\text{E}}^{\text{PH}}_{\text{i}}$) and chemical ($\dot{\text{E}}^{\text{CH}}_{\text{i}}$) exergy [9]. In this study, since there is no chemical reaction and the process is a separation, chemical exergy is avoided; therefore, the total exergy of the flows can be calculated according to Equation (9). On the other hand, physical exergy is obtained by multiplying the specific exergy ($\text{e}^{\text{PH}}_{\text{i}}$) at the mass flow rate ($\dot{\text{m}}_{\text{i}}$) of that flow (Equation 10). The specific exergy of each flow is read through the Span Haysys properties. Also, the amount of exergy loss in a thermodynamic system is calculated based on Equation (11) for each device ($\dot{\text{E}}^{\text{i}}_{\text{lost}}$) and according to Equation (12) for the whole process ($\dot{\text{E}}^{\text{total}}_{\text{lost}}$).

$$\dot{\text{E}}^{\text{i}}_{\text{Total}} = \dot{\text{E}}^{\text{PH}}_{\text{i}} + \dot{\text{E}}^{\text{CH}}_{\text{i}} = \dot{\text{E}}^{\text{PH}}_{\text{i}} \qquad (9)$$

$$\dot{\text{E}}^{\text{PH}}_{\text{i}} = \text{e}^{\text{PH}}_{\text{i}} \times \dot{\text{m}}_{\text{i}} \qquad (10)$$

$$\dot{\text{E}}^{\text{i}}_{\text{lost}} = \dot{\text{E}}^{\text{i}}_{\text{in}} - \dot{\text{E}}^{\text{i}}_{\text{out}} \qquad (11)$$

$$\dot{\text{E}}^{\text{total}}_{\text{lost}} = \dot{\text{E}}^{\text{total}}_{\text{in}} - \dot{\text{E}}^{\text{total}}_{\text{out}} \qquad (12)$$

In the current process, the total input and output exergy is obtained through equations (14) and (15) and its total exergy efficiency is obtained using equation (13), respectively. In addition, in the proposed design, with a slight change in the values related to the total input exergy and the total output of relations (17) and (18) and the amount of total exergy efficiency is also written based on relation (16). Also in Table (6) the relationships related to the input and output exergy of the equipment used in the dew point adjustment process are presented.

$$\eta^{\text{total}}_{\text{exergy}} = \frac{\dot{\text{W}}_{\text{Turbine}} + \dot{\text{E}}_{\text{Out Gas}} + \dot{\text{E}}_{36} + \dot{\text{E}}_{\text{Butane}} + \dot{\text{E}}_{\text{Propane}}}{\dot{\text{E}}_{\text{Dehyd Gas}} + \dot{\text{E}}_{\text{Rebs}} + \dot{\text{W}}_{\text{Air Coolers}} + \dot{\text{W}}_{\text{Comp}}} \qquad (13)$$

$$\dot{\text{E}}^{\text{total}}_{\text{in}} = \dot{\text{E}}_{\text{Dehyd Gas}} + \dot{\text{E}}_{\text{Rebs}} + \dot{\text{W}}_{\text{Air Coolers}} + \dot{\text{W}}_{\text{Comp}} \qquad (14)$$

$$\dot{\text{E}}^{\text{total}}_{\text{out}} = \dot{\text{W}}_{\text{Turbine}} + \dot{\text{E}}_{\text{Out Gas}} + \dot{\text{E}}_{36} + \dot{\text{E}}_{\text{Butane}} + \dot{\text{E}}_{\text{Propane}} \qquad (15)$$

$$\eta^{\text{total}}_{\text{exergy}} = \frac{\dot{\text{W}}_{\text{Turbine}} + \dot{\text{E}}_{\text{Out Gas}} + \dot{\text{E}}_{36} + \dot{\text{E}}_{\text{Propane}} + \dot{\text{E}}_{\text{Butane}}}{\dot{\text{E}}_{\text{Dehyd Gas}} + \dot{\text{E}}_{\text{Rebs}} + \dot{\text{W}}_{\text{Comp}}} \qquad (16)$$

$$\dot{E}_{in}^{total} = \dot{E}_{Dehyd\ Gas} + \dot{E}_{Rebs} + \dot{W}_{Comp} \quad (17)$$

$$\dot{E}_{out}^{total} = \dot{W}_{Turbine} + \dot{E}_{Out\ Gas} + \dot{E}_{36} + \dot{E}_{Propane} + \dot{E}_{Butane} \quad (18)$$

Table 6. Exergy equations and relations

Component	Exergy In	Exergy Out
105-E-101	$\dot{E}_{Gas} + \dot{E}_{17}$	$\dot{E}_{01} + \dot{E}_{Gas\ to\ Comp}$
105-E-102	$\dot{E}_{01} + \dot{E}_{12}$	$\dot{E}_{02} + \dot{E}_{13}$
105-E-103	$\dot{E}_{03} + \dot{E}_{07}$	$\dot{E}_{04} + \dot{E}_{08}$
105-D-101	$\dot{E}_{04}$	$\dot{E}_{05} + \dot{E}_{11}$
105-GX-101	$\dot{E}_{05}$	$\dot{W} + \dot{E}_{06}$
105-K-101	$\dot{W} + \dot{E}_{10}$	$\dot{E}_{17}$
105-D-102	$\dot{E}_{06}$	$\dot{E}_{07} + \dot{E}$
105-E-104	$\dot{E}_{13} + \dot{E}_{21}$	$\dot{E}_{14} + \dot{E}_{22}$
105-C-101	$\dot{E}_{Reb} + \dot{E}_{15} + \dot{E}_{14}$	$\dot{E}_{16} + \dot{E}_{21}$
105-C-201	$\dot{E}_{Reb} + \dot{W}_{Air\ cooler} + \dot{E}_{24}$	$\dot{E}_{Propane} + \dot{E}_{29}$
105-C-301	$\dot{E}_{Reb} + \dot{W}_{Air\ cooler} + \dot{E}_{30}$	$\dot{E}_{Butane} + \dot{E}_{36}$

Where, $\dot{E}_{Rebs}$ is Exergy of reboilers, $\dot{E}_{Out\ Gas}$ is exergy of waste gas production, $\dot{W}_{Turbine}$ is production work of gas expansion turbine, $\dot{W}_{Comp}$ is consumption of waste gas booster compressor, $\dot{E}_{Dehyd\ Gas}$ is exergy of feed gas and $\dot{W}_{Air\ Coolers}$ are the consumable work of air cooler fans (condensers).

9. Present and compare results

9.1.Result of optimal structure simulation

Figure (5) shows a schematic of the optimal structure simulation. Also in Table (7) the simulation results for process flows are reported. Considering that the proposed structure has been aimed at thermodynamic optimization; therefore, there is no change in the mass balance, so the results related to the mass balance in the base and optimal state are quite similar.

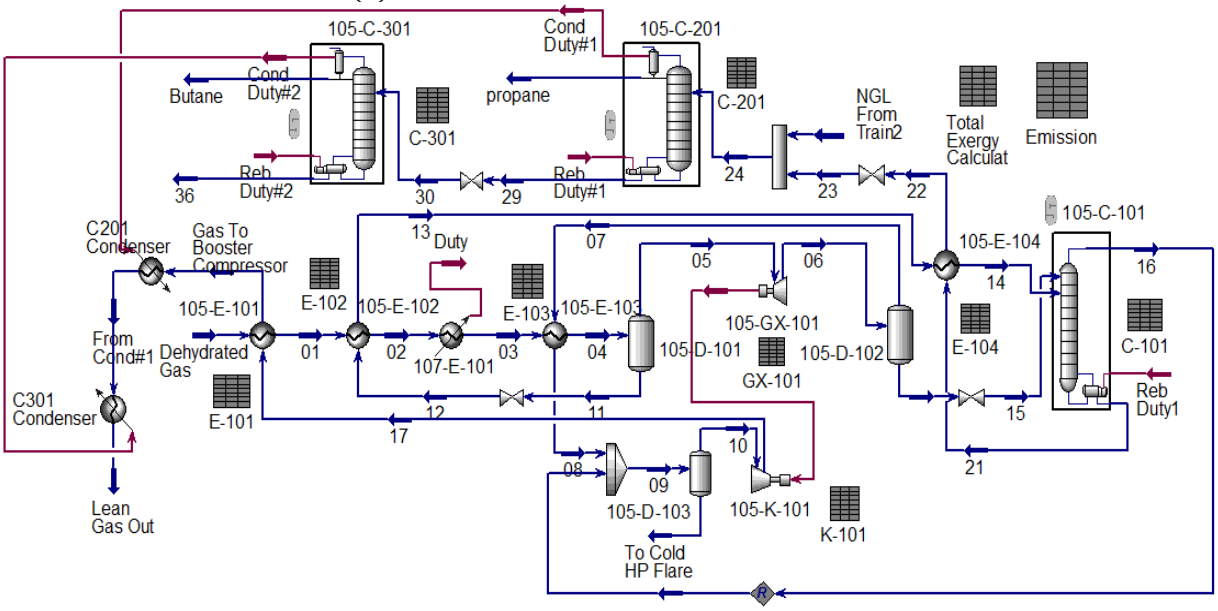

Fig. 5. Schematic of optimal structure simulation

Table 7. Information and specifications of optimal process flows

Stream	T (°C)	P (kPa)	F($\frac{kmole}{h}$)	stream	T (°C)	P (kPa)	F($\frac{kmole}{h}$)
Dehydrated Gas	25.9	7231	31660	01	13.6	7201	31660
03	-13.2	7091	31660	02	9.5	7141	31660
04	-31.8	7041	31660	05	-31.8	7041	30590
06	-66	3301	30590	07	-66.4	3301	28500
15	-67.9	3101	2087	13	5.8	3301	1074
10	-33	3101	30800	17	-7.4	4152	30800
09	-32.8	3101	30800	08	-35.13	3171	28500
16	-23.5	3101	2299	21	115.6	3141	861.2
22	54.6	2991	861.2	23	40.5	2221	861.2
24	40.4	2181	1729	propane	59.3	2201	764.3
29	134	2241	965	30	85.6	771.3	965
Butane	58	751.3	405.4	36	96.1	791.3	559.6
Lean out Gas	45.27	4191	30800	From Cond#1	26.23	4191	30800

9.2. Sensitivity analysis

In the dew point adjustment process, which has an expansion turbine, the outlet pressure of the turbine affects the whole process and affects the parameters of energy, exergy, carbon dioxide emission and production of gaseous liquids. Therefore, in this part of the research, the output pressure of the turbo-expander is considered as an independent variable and the changes of this parameter in the range of 2500 to 3500 kPa on other variables in the baseline and optimal process are investigated. According to Figures (6) to (8), increasing the outlet pressure of the turbo-expander has reduced the duty reboiler of the de-ethanizer, depropnazier and debuthanizer distillation towers. This downward trend is quite similar in the base and optimal state and has the same quantities.

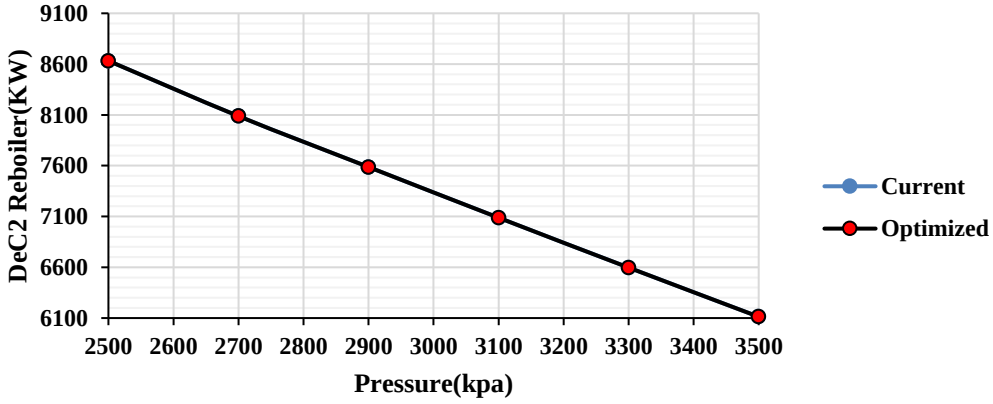

Fig. 6. Effect of expander outlet pressure on the de-ethanizer tower reboiler

This is because when the turbocharger pressure increases, the outlet temperature of this equipment also rises and as a result the distillation towers are fed with less intensity to separate ethane, propane, butane and condensate, so the towers for separation and Product recycling has to work with less duty, and there is a downward trend for all three ethanes, propanes and butanes distillation towers. Of course, as shown in Figures (6) to (8), the values for the current process and the optimum for the duty reboilers are exactly the same because of the effect of the optimization scenario

only on the condensers of the propagation distillation towers.

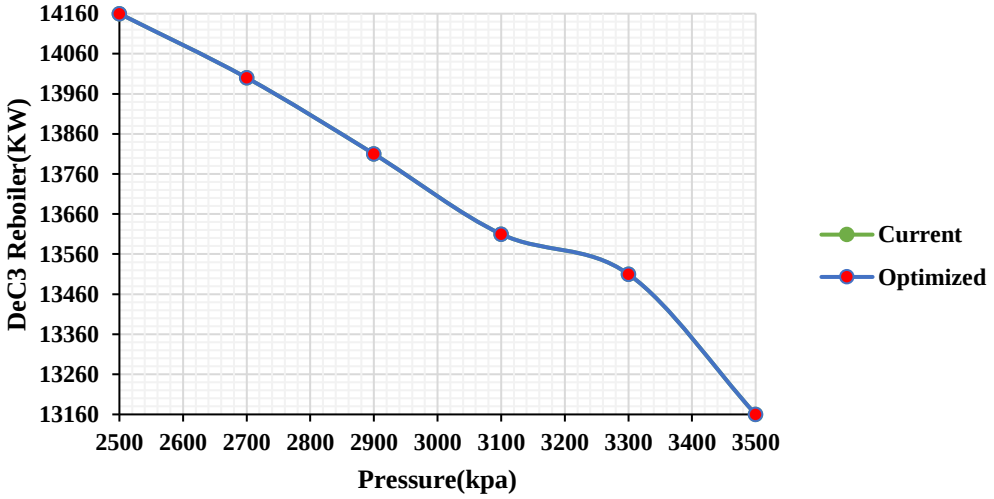

Fig. 7. Effect of expander outlet pressure on duty reboiling depropnazier tower

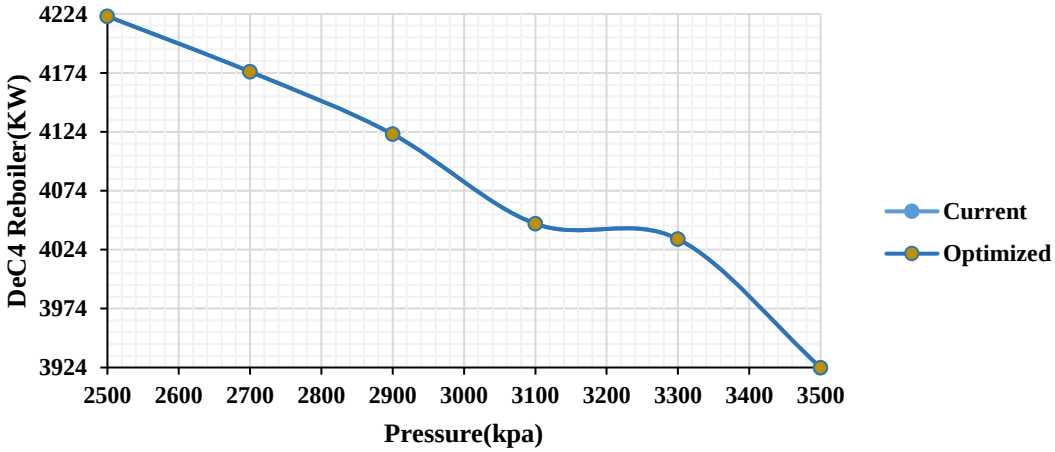

Fig. 8. Effect of expander outlet pressure on duty reboiling debuthanizer tower

According to Figure (9), when the expansion turbine is operating at a lower pressure, the gas-liquid flow rate is increased and more hydrocarbons are recovered. The turbo-expander is basically used to create refrigeration, to create an effective temperature drop with pressure drop, and to extract more hydrocarbons from natural gas.

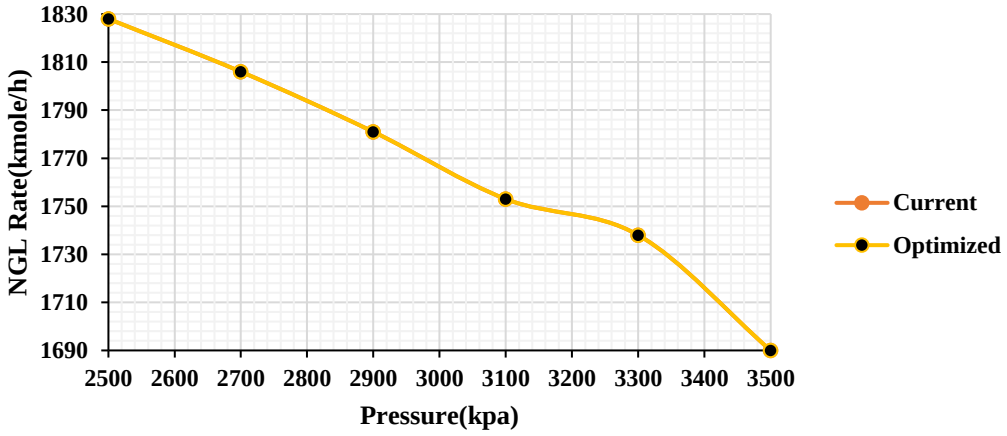

Fig. 9. Effect of expander outlet pressure on the intensity of gaseous liquid (NGL) production

According to Figure (10), the emission of carbon dioxide (total amount) is inversely related to the outlet pressure of the turbo-expander. By increasing the outlet pressure of the expansion turbine, as mentioned (Figure 10), the production of gaseous liquids will be less and as a result, the recovery of valuable hydrocarbons will be reduced. As a result, distillation towers are needed to recover ethane, propane, butane, and condensate to consume less duty, which makes the downward trend more pronounced for the optimal process; because in this case there are no condensers and due to the reduction of electricity consumption, the amount of carbon dioxide emissions has also decreased.

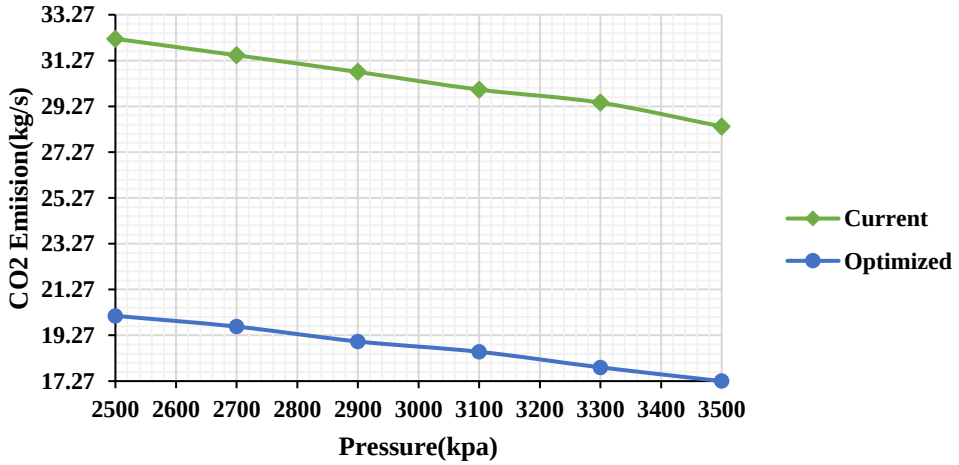

Fig. 10. The effect of expander outlet pressure on the overall emission of carbon dioxide

According to what is shown in Figure (11), with increasing the outlet pressure of the turbo expander, the overall exergy efficiency also increased. However, in general, Figure (11) shows that the optimal process has a higher exergy efficiency in all values. The reason for the increase in thermodynamic efficiency due to the increase in turbo-expander outlet pressure is, firstly, a decrease in the outlet fluid temperature and, secondly, less recovery from NGL. As NGL recovery decreases, existing distillation towers for hydrocarbon recovery should consume less duty (Figures 6 to 8), which increases the exergy efficiency. It should be noted that the high efficiency of exergy is the optimal process due to the removal of air conditioners (condensers, depropnazier and debuthanizer towers).

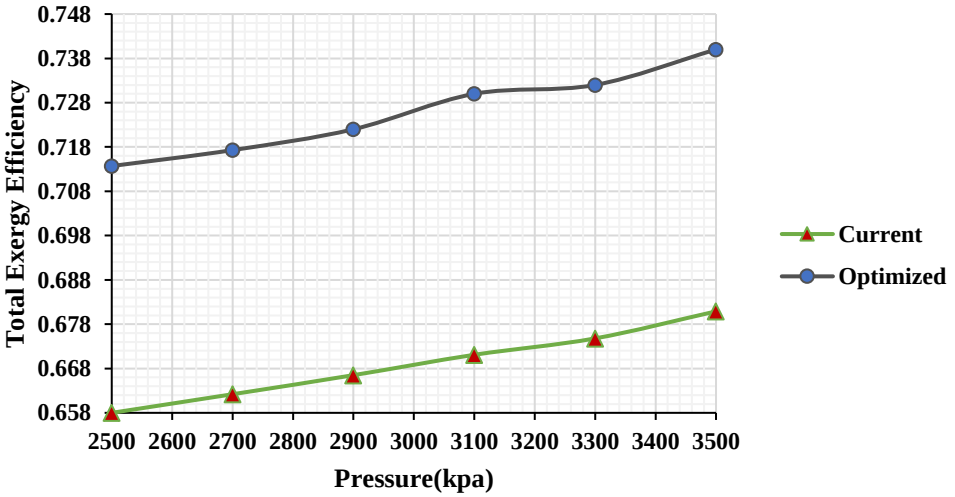

Fig. 11. Effect of expander outlet pressure on overall exergy efficiency

9.3. Energy and exergy evaluation results

Table (8) reports the values of the reboiler and condensers for the distillation columns in the current and optimal process. Based on these values, a parameter is defined as the intensity of hydrocarbon recovery energy (θ_{HCB}), which is written based on Equation (19):

$$\theta_{HCB}\left(\frac{kj}{kg_{prod}}\right)=\frac{\sum Duty}{\dot{m}_i} \qquad (19)$$

Where, $\sum Duty$ is the consumption of duty required for the recovery of hydrocarbons, the value of which is given in Table (8) for the current and optimal process. $\dot{m}_i$ is a mass flow in terms of $(\frac{kg}{h})$ component i, which in this paper is related to propane, butane and condensate. Accordingly, the amounts of energy required to recover hydrocarbons are calculated and shown in Table (8). According to Equation (19), the total duty consumption for propane production is the sum of the duty reboiler and condenser of the de-ethanizer and depropnazier towers (current process) and in the optimal case, the amount of condensate is removed.Likewise, for the production of butane and condensate, the total consumption of the duty equal to the sum of the diuretics of the reboiler and condenser towers of de-ethanizer, depropnazier and debuthanizer (current process) and in the optimal case the amount of electricity consumed in both condensers has been eliminated.

Table 8. Duty consumption (KW) of distillation towers in the current and optimal process

Subject	Current process	Optimized process
Duty reboiler de-ethanizer tower	6592	6592
Duty reboiler depropnazier tower	13440	13440
Electricity consumption of Condensing depropnazier tower	8402	0
Duty reboiler debuthanizer tower	4015	4015
Electricity consumption of Condensing debuthanizer tower	6898	0
Total consumption	39347	24047
Intensity of consumption for propane product$(\frac{kj}{kg_{prod}})$	3057/42	2154
Intensity of consumption for butane product$(\frac{kj}{kg_{prod}})$	6048/22	3696/38
Intensity of consumption for condensate product$(\frac{kj}{kg_{prod}})$	3480/32	2127

Figures (12) and (13) show the effect of the optimization scenario on the thermodynamic improvement of distillation towers. According to Figure (12), the duty consumption of the de-ethanizer distillation tower is the same for both cases, but in the depropnazier and debuthanizer distillation towers, the conditions are completely in favor of the proposed scenario. According to Figure (12), the total duty of depropnazier and debuthanizer distillation towers in the optimal process is 61.53 and 36.8% less than the current process, respectively. Also, according to the study, the total duty consumed in the optimal process is 38.88% less than the base state. According to Figure (13), the optimal process was able to use less energy to recover all the hydrocarbons produced. This is clearly seen in Figure (13). Based on this figure, in general, the recovery energy for butane from the two products of propane and condensate is more, the recovery energy for the propane product is less than the others. According to the comparison, the recovery intensities of propane, butane and condensate in the optimal process are 29.55, 38.88 and 38.88 percent lower than the current state, respectively.

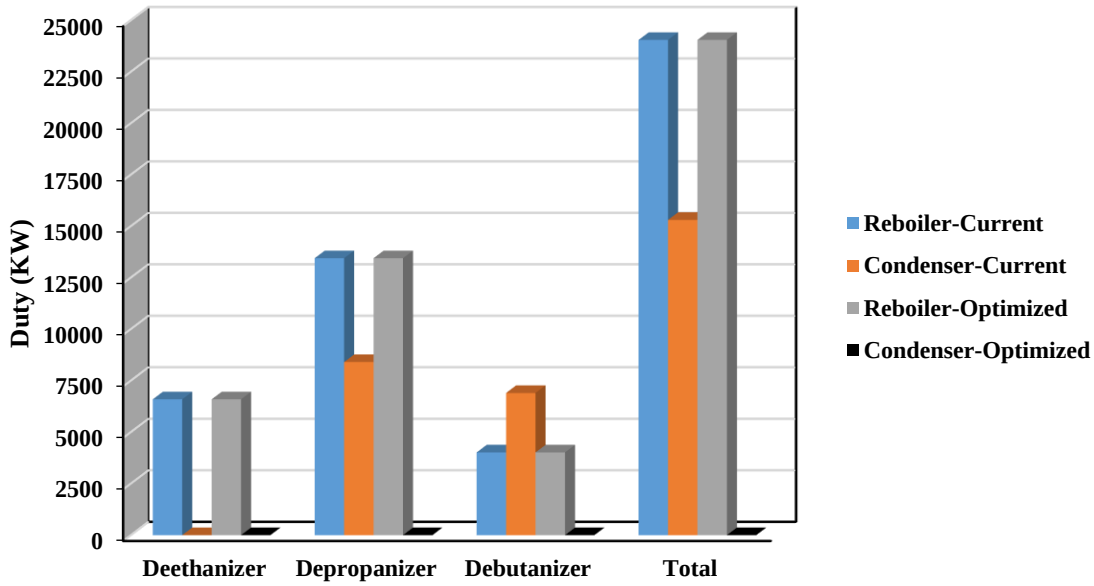

Fig. 12. Comparison of distillation towers in the distillation and separation section for the current and optimal process

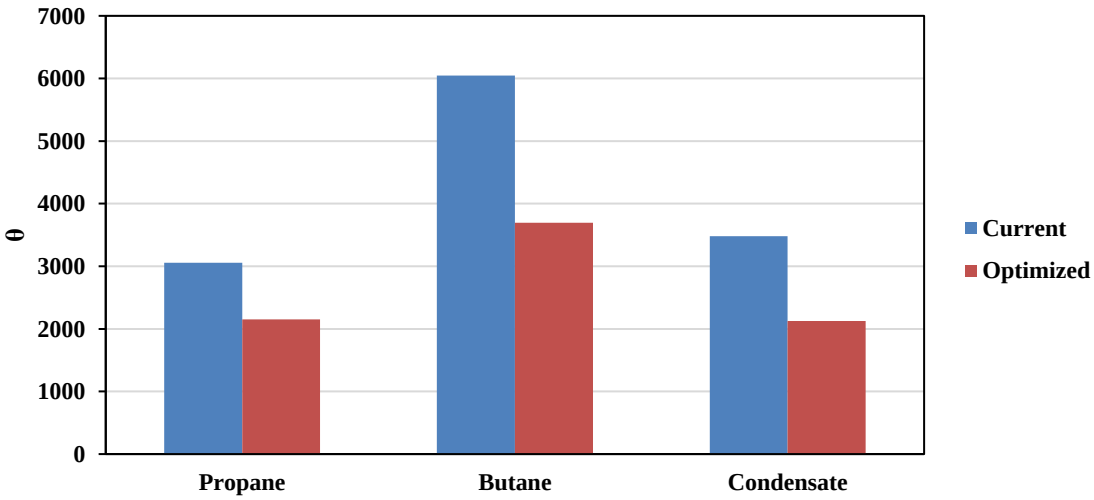

Fig. 13. Comparison of the intensity of hydrocarbon recovery energy in the current and optimal process

Tables (9) and (10) report exergy calculations for the current trend and the optimal process, respectively. According to Figure (14), the highest share of exergy loss in the current process is 41%, which is related to the C-201 distillation column. Among the distillation towers according to figure (14), the de-ethanolizer column has the lowest exergy loss, which can be explained by the use of the E-104 heat exchanger in which by preheating the feed, increases the thermodynamic efficiency of the tower. According to Figure (15) in the optimal process, C-201 distillation column has the highest exergy loss, with the difference that the loss percentage here is 37%, which is 4% less than the current process. Also, the increase of thermodynamic efficiency for the debuthanizer tower in the optimal process is quite evident.

Table 9. Exergy calculations for the current process

Equipments	$\dot{E}^{i}_{in}$**(KW)**	$\dot{E}^{i}_{out}$**(KW)**	$\dot{E}^{i}_{lost}$**(KW)**
105-E-101	166500	33/166083	67/416
105-E-102	22/91472	56/91055	66/416
105-E-103	67/162126	56/160555	11/1571
105-GX-101	56/88805	78/86027	78/2777
105-K-101	79250	33/77583	67/1666
105-E-104	3375	56/3030	44/344
105-C-101	22/13422	22/6572	6850
105-C-201	44/17244	2340	44/14904
105-C-301	67/7866	67/561	7305
η^{total}_{exergy}		6754/0	

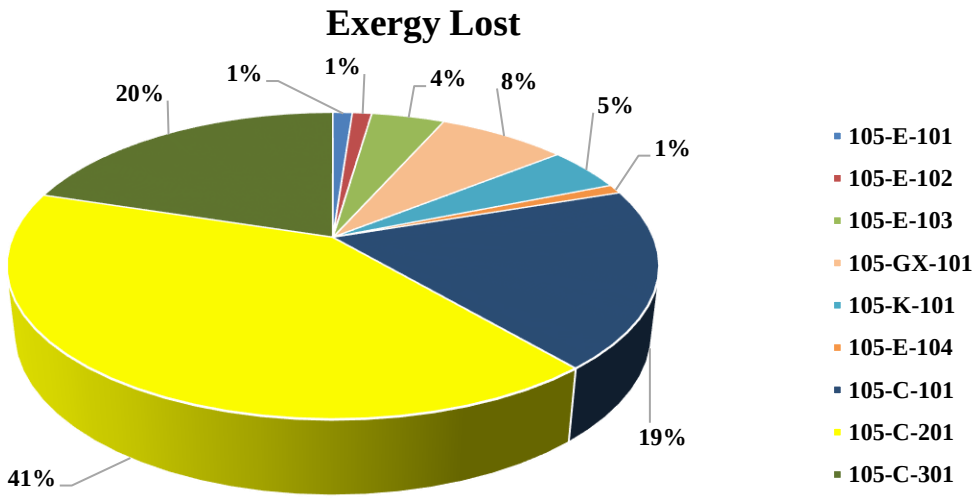

Fig. 14. The share of equipment exergy loss in the current process

Based on the comparison of Figures (14) and (15), the share of exergy loss of this tower in the current process is 20% and in the optimized process is 12%. In the current process, due to the use of air conditioners as condensers, the exergy loss is greater than the optimal process, and this is the result of the exergy calculations. According to Figure (16) and Tables (9) and (10), the exergy loss in the distillation towers of depropnazier, debuthanizer and the whole system in the optimal process are 32.48, 54.19 and 27/27, respectively and it is 24% less than the current trend.

Table 10. Exergy calculations for optimal process

Equipments	$\dot{E}^{i}_{in}$(KW)	$\dot{E}^{i}_{out}$(KW)	$\dot{E}^{i}_{lost}$(KW)
105-E-101	166500	166083/33	416/67
105-E-102	91472/22	91055/56	416/66
105-E-103	162126/67	160555/56	1571/11
105-GX-101	88805/56	86027/78	2777/78
105-K-101	79250	77583/33	1666/67
105-E-104	3375	3030/56	344/44
105-C-101	13422/22	6572/22	6850
105-C-201	12402/78	2340	10062/78
105-C-301	3908/33	561/67	3346/66
η^{total}_{exergy}		0/7305	

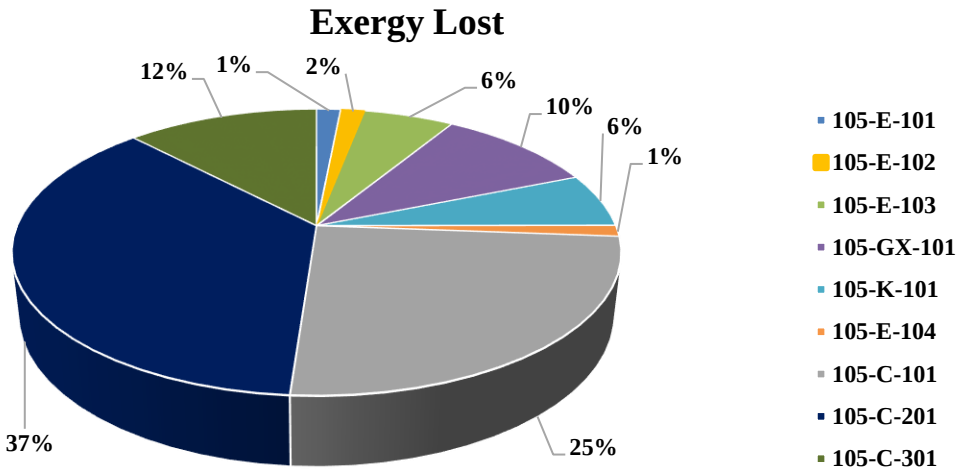

Fig. 15. Contribution of equipment exergy loss in the optimal process

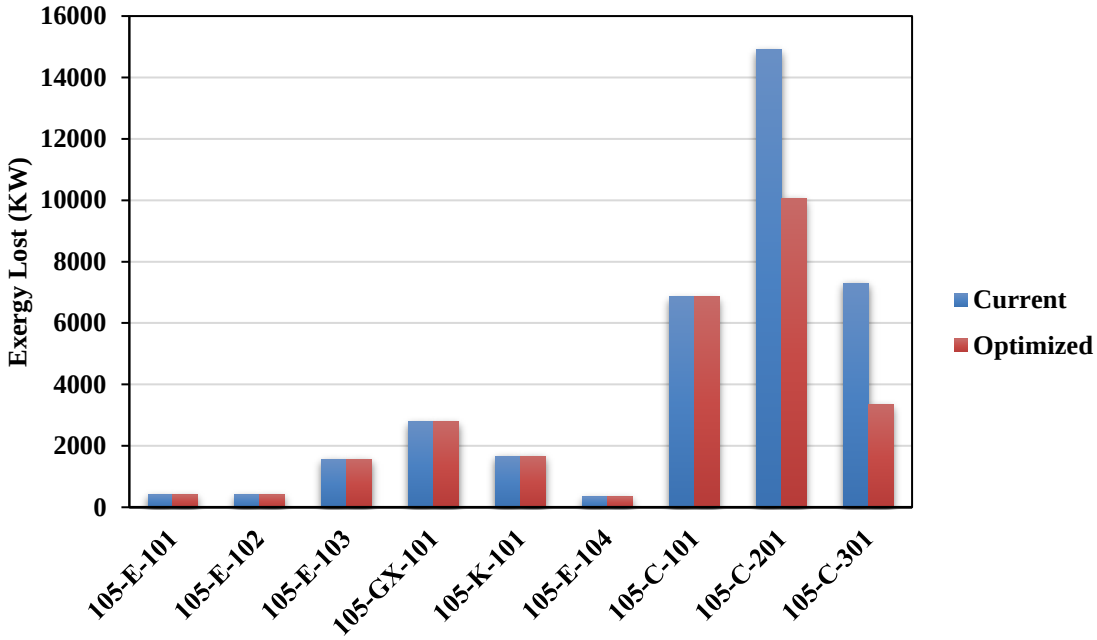

Fig. 16. Comparison of equipment exergy loss in optimal and current process

9.4. Results of economic analysis

In this section, the results obtained from the economic evaluation are presented. The results of basic calculations (direct, indirect costs, fixed costs and investment) for the current and optimal process are reported in Tables (11) and (12), respectively. In addition, these results are compared in Figure 17. According to the comparison, the cost of investing in the optimal process is 1% lower than the current trend.

Table 11. Basic economic calculations for the current process.

I.Fixed-Capital Investment (FCI)	
A. Direct Costs (DC)	
A.1. Onsite Costs (ONSC)	
Purchased-Equipment Cost (PEC)	5166500
Purchased-Equipment installation	4649850
Piping	3616550
Instrumentation and Controls	2066600
Electrical Equipment and materials	774975
A.2. Offsite Costs (OFSC)	
Land	516650
Civil, structural and architrctural work	4649850
Service facilities	5166500
Total direct costs (DC) = 26607475	
B. Indirect Costs (IC)	
B.1. Engineering and supervision	3874875
B.2. Construction costs	3991121.25
B.3. Contingencies	1966499.06

Total indirect costs (IC) = 9832495.31	
Total Fixed Capital Investment (FCI) = 36439970.31	
II. Other Outlays	
Startup costs	4372796.44
Working capital	11569690.58
Allowance for funds used during construction	5465995.55
Total Capital Investment (TCI) = 57848452.88	

Table 12. Basic economic calculations for the optimal process

I.Fixed-Capital Investment (FCI)	
A. Direct Costs (DC)	
A.1. Onsite Costs (ONSC)	
Purchased-Equipment Cost (PEC)	5119400
Purchased-Equipment installation	4607460
Piping	3583580
Instrumentation and Controls	2047760
Electrical Equipment and materials	767910
A.2. Offsite Costs (OFSC)	
Land	511940
Civil, structural and architrctural work	4607460
Service facilities	5119400
Total direct costs (DC) = 26364910	
B. Indirect Costs (IC)	
B.1. Engineering and supervision	3839550
B.2. Construction costs	3954736.5
B.3. Contingencies	1948571.63
Total indirect costs (IC) = 9742858.13	
Total Fixed Capital Investment (FCI) = 36107768.13	
II. Other Outlays	
Startup costs	4332932.18
Working capital	11464216.38
Allowance for funds used during construction	5416165.22
Total Capital Investment (TCI) = 57321082	

After performing economic calculations for the optimal process and the current trend, the results of economic estimation in the form of investment cost, energy cost, total annual cost and production cost of gaseous liquids, the results are presented in Table (13) and together in Figure (17). Based on the comparison, it was found that the energy cost of the optimal process is 27% lower than the current trend, which, taking into account this amount of the optimal process and it saves 31,575,494 $ annually in the energy supply sector.

Table 13. Results of economic estimation

Current process	
Investment cost	88/57848452
Energy cost	11506200
Total annual cost	63/30789017
NGL production cost	039/0
Optimized process	
Investment cost(dollar)	57321082
Energy cost(dollar in year)	55/8398650
Total annual cost(dollar)	22/10309011
NGL production cost($\frac{\$}{kg_{NGL}}$)	0345/0

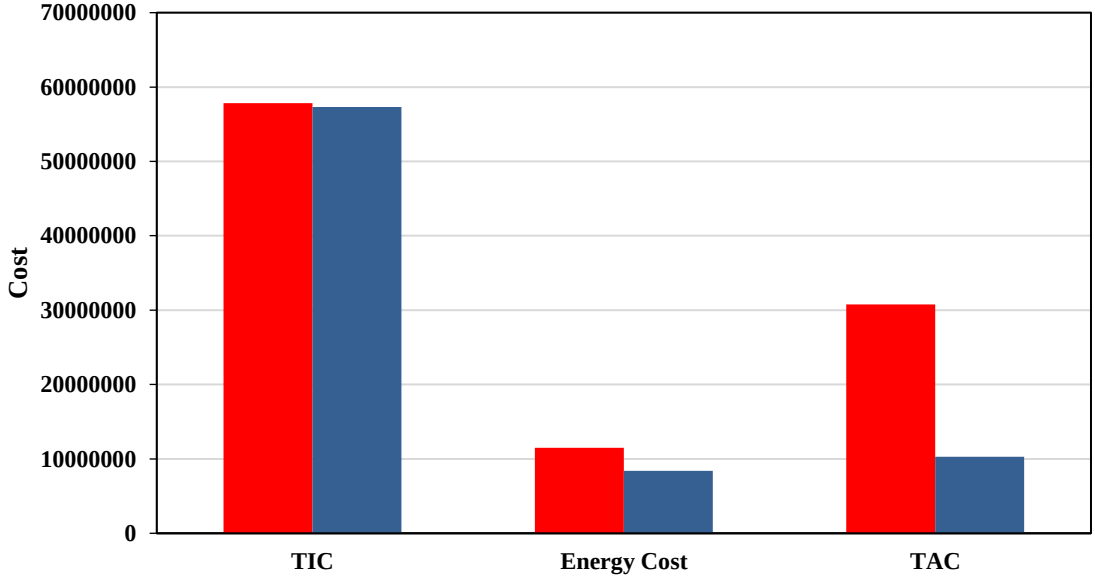

Fig. 17. Comparison of current and optimal process economic estimation result

Similarly, a comparison of the total annual cost and production cost of NGL product was performed and it was found that the optimal process has a significant advantage in this regard and 66.52% in the annual cost of the process has been reduced. Finally, economic analysis showed that in the optimal process, the cost of production of NGL product was $0.0345\frac{\$}{kg_{NGL}}$, which shows a decrease of 11.54% in this sector compared to the baseline.

9.5. Results of carbon dioxide emission analysis

Tables (14) and (15) show the calculations of carbon dioxide emissions in the current and optimal process. According to these tables, the total emission of carbon dioxide is 29.31 $\frac{kg}{s}$for the base condition and 17.91 $\frac{kg}{s}$ for the optimal process.

Table 14. Evaluation of carbon dioxide emissions ($\frac{kg}{s}$) through the current process

Parameter	Amount
Emission through reboiler of de-ethanizer tower	4/91
Emission through reboiler of depropnazier tower	10/01
Emission through reboiler of debuthanizer tower	2/99
Emission through the air conditioning of depropnazier tower	6/26
Emission through the air conditioning of debuthanizer tower	5/14
Total emission through the electricity support service	11/4
Total emission through the steam support service	17/91

Total emission	29/31

Table 15. Evaluation of carbon dioxide ($\frac{kg}{s}$) emission through optimal process

Parameter	Value
Emission through reboiler of de-ethanizer tower	4/91
Emission through reboiler of depropnazier tower	10/01
Emission through reboiler of debuthanizer tower	2/99
Emission through the air conditioning of depropnazier tower	0
Emission through the air conditioning of debuthanizer tower	0
Total emission through the electricity support service	0
Total emission through the steam support service	17/91
Total emission	17/91

According to Figure (18), the highest emission rate for the propulsion tower (reboiler) is in the current process and the emission share in this section is 34%. Also, according to Tables (14) and (15), the share of emission through electricity and steam utility for the current process is 38.9 and 61.1%, and for the optimal process, all emission is through steam utility and emission through electricity is 0%.

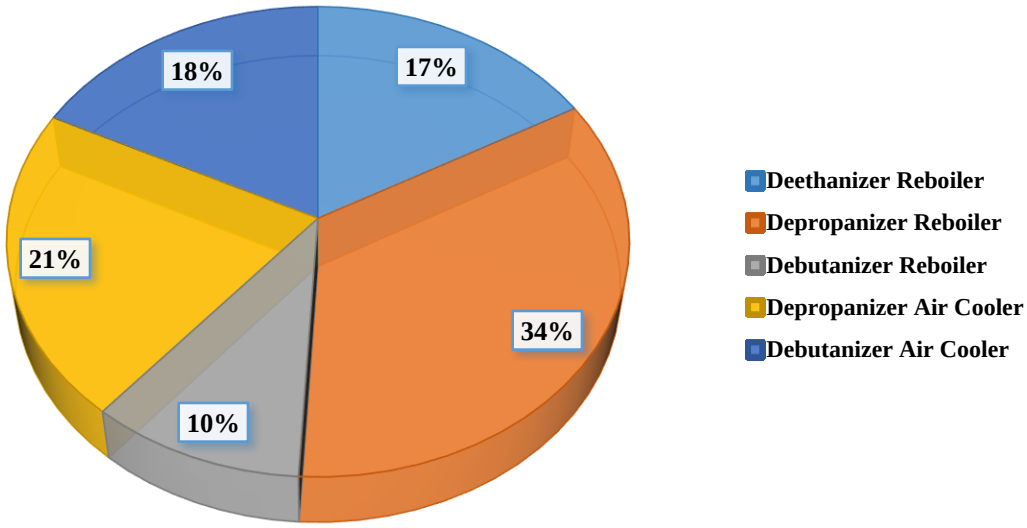

Fig. 18. Comparison of the share of different segments in the current process

Figure (19) shows that in the optimal process there is no share of emission through electricity utility and this leads to a reduction of 38.9% of the total emission compared to the baseline mode. By removing the air conditioners and replacing them with heat exchangers, the condensation has been practically through integration, which has reduced the total fuel consumption in the utility supply section for the fans related to the air conditioners. However, according to Figure (19), the share of carbon dioxide emissions in the reboiler section of the propulsion tower is higher than other section which is equal to 56%, which shows that in total, the distillation tower had the highest utility demand.Table (16) shows a comparison of the results of carbon emission analysis for the current and optimal process. According to this table, considering the effect of the proposed scenario on air conditioners, the distillation towers have been depropnazier and debuthanizer depleted; Therefore, there is no significant difference in the amount of emission through reboilers and is equal to 17.91 $\frac{kg}{s}$. In addition, the amount of carbon dioxide footprint in the optimal

process according to Table (16) is significantly lower than the current trend. Analyzes show that in the optimal process, the production of NGL is 1.33 kg of carbon dioxide released per kilogram of product, which shows a decrease of 39% compared to the current trend.

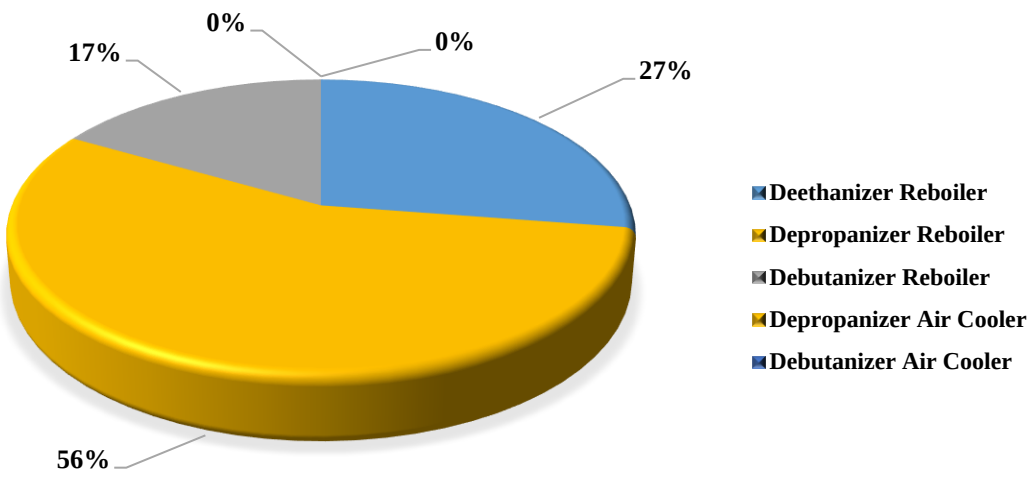

Fig. 19. Comparison of the contribution of different sections in the optimal process

Table 16. Comparison of carbon dioxide emission results

Subject	Current process	Optimal process
Emission through electricity($\frac{kg}{s}$)	11/4	0
Emission through steam($\frac{kg}{s}$)	17/91	17/91
Total emission($\frac{kg}{s}$)	29/31	17/91
Carbon di oxide footprint($\frac{kg_{CO_2}}{kg_{NGL}}$)	2/18	1/33

10. Conclusion

The term thermal integration in this study has two meanings. First, it deals with the physical arrangement of equipment, process parts, in terms of central heating or cooling. Second, with methods and auxiliary tools aimed at increasing energy efficiency in the existing dew point regulation unit points to a range of process synthesis. Such an improvement in energy efficiency can be achieved by combining heating and cooling requirements and thus reducing the need for external heating and cooling equipment (external means the same as support services).

The dew point adjustment process using turbo expansion has provided a high potential for energy integration and in this paper this potential has been used the most. Studies have shown that by using the proposed scenario in this article, the following benefits can be achieved:

1. Thermodynamic improvement
2. Reduce the overall annual cost
3. Reduce the cost of producing a product with NGL value

The integration of energy in the dew point adjustment unit is fortunately economically justified, and this is evident from the economic assessment. The proposed scenario operates in a way that enhances the existing process in all sectors (energy, exergy, economic and environmental). With the removal of air conditioners, a significant amount of the system's need for utility has been reduced, and since energy, economy and environment are inseparable, with the implementation of the proposed plan, its efficiency will be determined in the short term and completely benefit the process. Sensitivity analysis showed that the output pressure parameter of the turbo-expander is a very important factor in the thermodynamic changes

of the dew point adjustment process. Studies have shown that increasing this parameter will increase the overall exergy efficiency, reduce product production and reduce energy consumption in distillation tower reboilers. In this operating unit, the focus of thermal integration has been to eliminate air conditioners, and thus two process-process heat exchangers have been replaced. However, according to the exergy assessment, there is still a loss of exergy in this process and the largest share is related to the depropnazier distillation tower.From the environmental point of view, it was found that in the current process, the total amount of carbon dioxide emissions per recovered gaseous liquid is high, but the proposed scenario has taken a very positive step in reducing this amount. Considering that the sixth refinery of South Pars has used part of its refined gas as fuel for utility supply units, as a result of implementing the proposed scenario, a significant volume of gas fuel can be saved and Turn the production cycle in the global gas network.Finally, it can be said that the proposed scenario is a suitable alternative to the current process of the dew point adjustment unit of the sixth phase of the South Pars refinery. Carrying out this project due to the reduction of carbon dioxide emissions will lead to a positive outlook for this refinery in the public mind and will reduce the level of pollution in the South Pars energy region. Also, based on economic assessments, the proposed process will reduce the cost of investment and production costs of hydrocarbon products.

REFERENCES

[1] Fahmy MFM, Nabih HI, El-Rasoul TA. Optimization and comparative analysis of LNG regasification processes. Energy. 2015; 91:371-85.

[2] Aslani A, Akbari S, Tabasi S. The Robustness of Natural Gas Energy Supply: System Dynamics Modelling. International Journal of System Dynamics Applications (IJSDA). 2018;7(3):57-71.

[3] Ghorbani B, Mehrpooya M, Omid E. Hybrid solar liquefied natural gas, post combustion carbon dioxide capture and liquefaction. Energy Convers Manage 2020; 207:112512.

[4] Ghorbani B, Shirmohammadi R, Mehrpooya M. A novel energy efficient LNG/NGL recovery process using absorption and mixed refrigerant refrigeration cycles – Economic and exergy analyses. Appl Therm Eng 2018; 132:283–95.

[5] V. Zare, S.M.S. Mahmoudi, A thermodynamic comparison between organic rankine and kalina cycles for waste heat recovery from the gas turbine-modular helium reactor, Energy. 79 (2015) 398–406. doi:10.1016/j.energy.2014.11.026.

[6]Y. Cao, Y. Gao, Y. Zheng, Y. Dai, Optimum design and thermodynamic analysis of a gas turbine and ORC combined cycle with recuperators, Energy Convers. Manag. 116 (2016) 32–41. doi:10.1016/j.enconman.2016.02.073.

[7]Y. Han, G. Xu, Q. Zheng, C. Xu, Y. Hu, Y. Yang, et al., New heat integration system with bypass flue based on the rational utilization of low-grade extraction steam in a coal-fired power plant, Appl. Therm. Eng. 113 (2017) 460–471. doi:10.1016/j.applthermaleng.2016.11.056.

[8] S.-C. Yang, T.-C. Hung, Y.-Q. Feng, C.-J. Wu, K.-W. Wong, K.-C. Huang, Experimental investigation on a 3kW organic Rankine cycle for low-grade waste heat under different operation parameters, Appl. Therm. Eng. 113 (2017) 756–764. doi:10.1016/j.applthermaleng.2016.11.032.

[9] S. Zhao, S. Yan, D.K. Wang, Y. Wei, H. Qi, T. Wu, et al., Simultaneous heat and water recovery from flue gas by membrane condensation: Experimental investigation, Appl. Therm. Eng. 113 (2017) 843–850.doi:10.1016/j.applthermaleng.2016.11.101.

[10]Finn, A.J., Tomlinson, T.R., Johnson, G.L., Modern process designs for very high NGL recovery. In: GPA Annual Convention Proceedings. 1999; 308e314.

[11]Makitan, V., Huang, S., Gerdes, K., Impact of pressure recovery on C2 recovery processes - Comparing performances between expander and JT valves. In: 2010 AIChE Spring Meeting and 6th Global Congress on Process Safety.

[12]Jibril, K.L., Al-Humaizi, A.I., Idriss, A.A., Ibrahi, A.A., 2005. Simulation of turboexpander processes for recovering of natural gas liquids from natural gas. Saudi Aramco Journal of Technology, 9e14.

[13]H.M. Hudson, J.D. Wilkinson, J.T. Lynch, R.N. Pitman, M.C. Pierce, Reducing treating requirements for cryogenic NLG recovery plants, in: 80th Annual Convention of the Gas Processors Association, San Antonio, TX, March 12, 2001.

[14] J.T. Lynch, J.D. Wilkinson, H.M. Hudson, R.N. Pitman, Process retrofits maximize the value of existing NGL and LPG recovery plants, in: 82nd

Annual Convention of the Gas Processors Association, San Antonio, TX, 2003.
[15] C.W. Kim, S.D. Chang, S.T. Ro, Analysis of the power cycle utilizing the cold energy of LNG, International Journal of Energy Research 19 (1995) 741–749.
[16] G.S. Lee, Y.S. Chang, M.S. Kim, S.T. Ro, Thermodynamic analysis of extraction processes for the utilization of LNG cold energy, Cryogenics 36 (1996) 35–40.
[17] T. Miyazaki, A. Akisawa, T. Kashiwagi, LNG cold energy cycle, in: Proceedings of the JSRAE, 1998, pp. 57–160.
[18] S. Deng, H.J. Ruixian Cai, R. Lin, Novel cogeneration power system with liquefied natural gas (LNG) cryogenic exergy utilization, Energy 29 (2004) 497–512.
[19] P.H. Wei Sun, Zeshao Chen, Lei Jia, Performance of cryogenic thermoelectric generators in LNG cold energy utilization, Energy Conversion and Management 46 (2005) 789–796.
[20] M. Mehrpooya, F. Gharagheizi, A. Vatani, An optimization of capital and operating alternatives in a NGL recovery unit, Chem. Eng. Technol. 29 (2006) 1469–1480.
[21] GPSA Engineering Data Book, 11th ed., Vol. 1-2, Gas Processors Suppliers Association, Tulsa, Oklahoma, 1998.
[22] M. Mehrpooya, A. Vatani, S.M.A. Mousavian, Introducing a novel integrated NGL recovery process configuration (with a self-refrigeration system (openclosed cycle) with minimum energy requirement, Chem. Eng. Process. 49 (2010) 376–388.
[23] R. Lee, Y. Jame, J.J.Y, D. Elliot, Internal refrigeration for enhanced NGL recovery, U.S. Patent, vol. 150, 2006, p. 672.
[24] M. Mehrpooya, A. Vatani, S. Mousavian, Optimum design of integrated liquid recovery plants by variable population size genetic algorithm, Can. J. Chem. Eng. 88 (2010) 1054–1064.
[25] B. Ghorbani, M. Mafi, R. Shirmohammadi, M. Hamedi, M. Amidpour, Optimization of operation parameters of refrigeration cycle using particle swarm and NLP techniques, Nat. Gas. Sci. Eng 21 (2014) 779–790.
[26] B. Ghorbani, M. Hamedi, M. Amidpour, M. Mehrpooya, Cascade refrigeration systems in integrated cryogenic natural gas process (natural gas liquids (NGL), liquefied natural gas (LNG) and nitrogen rejection unit (NRU)), Energy 115 (2016) 88–106.
[27] B. Ghorbani, M. Mehrpooya, M. Hamedi, M. Amidpour, Exergoeconomic analysis of integrated natural gas liquids (NGL) and liquefied natural gas (LNG) processes, Appl. Therm. Eng. 113 (2017) 1483–1495.
[28] B. Ghorbani, M. Hamedi, M. Amidpour, R. Shirmohammadi, Implementing absorption refrigeration cycle in lieu of DMR and C3MR cycles in the integrated NGL, LNG and NRU unit, Int. J. Refrig 77 (2017) 20–38.
[29] B. Ghorbani, R. Shirmohammadi, M. Mehrpooya, A novel energy efficient LNG/NGL recovery process using absorption and mixed refrigerant refrigeration cycles–Economic and exergy analyses, Appl. Therm. Eng. 132 (2018) 283–295.
[30] M. Mehrpooya, F. Gharagheizi, A. Vatani, Thermoeconomic analysis of a large industrial propane refrigeration cycle used in NGL recovery plant, Int. J. Energy Res. 33 (2009) 960–977.
[31] E. Konukman, A. Akman, Flexibility and operability analysis of a HEN-integrated natural gas expander plant, Chem. Eng. Sci. 60 (2005) 7057–7074.
[32]W. Jang, J. Hahn, R. Hall, Genetic/quadratic algorithm for plant economic optimizations using a process simulator, Comput. Chem. Eng. 30 (2005) 285–294.
[33] Engineering Data Book, Refrigeration, 12th ed., Gas Processors Supply Association, Tulsa, OK, Sec. 16, 2004.
[34] M. Mehrpooya, A. Jarrahian, M. Pishvaie, Simulation and exergy-method analysis of an industrial refrigeration cycle used in NGL recovery units, Int. J. Energy Res. 30 (2006) 1336–1351.
[35] B. Tirandazi, M. Mehrpooya, A. Vatani, S. Moosavian, Exergy analysis of C2+ recovery plants refrigeration cycle, Chem. Eng. Res. Des. 89 (2011) 676–689.
[36] A. Vatani, M. Mehrpooya, B. Tirandazi, A novel process configuration for co-production of NGL and LNG with low energy requirement, Chem. Eng. Process. Process Intensif. 63 (2013) 16–24.
[37] J. Mak, S. Ana, C. Graham, Configuration and methods of integrated NGL recovery and LNG liquefaction. US 2007/0157663A1, 2007.
[38]W. Ransbarger, Intermediate pressure LNG refluxed NGL recovery process. US 2008/0098770 A1.

[39]R. Campbell, J. Wilkinson, H. Hudson, K. Cuellar, LNG production in cryogenic natural gas processing plants. US 6526777 B1, 2003.

[40] F. Nogal, S.P.J. Kim, S. Robin, Optimal design of mixed refrigerant cycles, Ind. Eng. Chem. Res. 47 (2008) 8724–8740.

[41] A. Alabdulkarem, A. Mortazavi, Y. Hwanga, R. Radermacher, P. Rogers, Optimization of propane pre-cooled mixed refrigerant LNG plant, Appl. Therm. Eng. 31 (2011) 1091–1098.

[42] M. Mehrpooya, A. Vatani, S.M.A. Mousavian, Introducing a novel integrated NGL recovery process configuration (with a self-refrigeration system (open closed cycle) with minimum energy requirement, Chemical Engineering and Processing 49 (2010) 376–388.

[43] Boehme R, Parise J, Pitanga Marques R. Simulation of multistream plateefin heat exchangers of an air separation unit. Cryogenics 2003;43:325e34.

[44] Miller J, Luyben WL, Belanger P, Blouin S, Megan L. Improving agility of cryogenic air separation plants. Ind Eng Chem Res 2008;47:394e404.

[45] Seliger B, Hanke-Rauschenbach R, Hannemann F, Sundmacher K. Modelling and dynamics of an air separation rectification column as part of an IGCC power plant. Sep Purif Technol 2006;49:136e48.

[46]Kansha Y, Tsuru N, Fushimi C, Shimogawara K, Tsutsumi A. An innovative modularity of heat circulation for fractional distillation. Chem Eng Sci 2010;65:330e4.

[47] Kansha Y, Tsuru N, Fushimi C, Tsutsumi A. Integrated process module for distillation processes based on self-heat recuperation technology. J Chem Eng Jpn 2010;43:502e7.

[48] Kansha Y, Tsuru N, Sato K, Fushimi C, Tsutsumi A. Self-heat recuperation technology for energy saving in chemical processes. Ind Eng Chem Res 2009;48:7682e6.

[49] BianS,Khowinij S,HensonMA,Belanger P,MeganL. high purity air separation columns. Comput ChemEng 2005;29:2096e109.

[50] Roffel B, Betlem B, De Ruijter J. First principles dynamic modeling and multivariable control of a cryogenic distillation process. Comput Chem Eng 2000;24:111e23.

[51] Asalooye Gas Refinery Data from South-Pars Gas Company, 2019. Asalooye, Iran.

[52]ASPEN Technology, 2017. Aspen Hysys. A User Guide Manual for Aspen Physical Property V10. Aspen Technology, Inc. Cambridge, MA.

[53]Rafael Oliveira dos Santos, Lizandro de Sousa Santos, Diego Martinez Prata," Simulation and optimization of a methanol synthesis process from different biogas sources", Journal of Cleaner Production 186 (2018).

[54]A. Nemati Rouzbahani , M. Bahmani , J. Shariati , T. Tohidian, M.R. Rahimpour, "Simulation, optimization, and sensitivity analysis of a natural gas dehydration unit", Journal of Natural Gas Science and Engineering 21 (2014) 159-169.

[55]William L, Luyben, Principles and case studies of simultaneous design, Published by John Wiley & Sons, Inc., Hoboken, New Jersey Published simultaneously in Canada (2010).

[56]Mehrnoosh Sarcheshmehpoor," Evaluation of a gas refinery using exergy-based methods," zur Erlangung des akademischen Grades, Berlin (2019).

[57]Omar Y. Abdelaziz, Wafaa M. Hosny, Mamdouh A. Gadalla, Fatma H. Ashour, Ibrahim A. Ashour, Christian P. Hulteberg," Novel process technologies for conversion of carbon dioxide from industrial flue gas streams into methanol", Journal of CO_2 Utilization 21 (2017) 52–63.

[58] Tsatsaronis G, Bejan A, Mamut E (eds) (1999) Strengths and limitations of exergy analysis. In: Thermodynamic Optimization of Complex Energy Systems. Kluwer Academic Publishers, Dordrecht, p 93-100.

[59].Siyu Yang, Qingchun Yang, Hengchong Li, Xing Jin, Xiuxi Li, and Yu Qian," An Integrated Framework for Modeling, Synthesis, Analysis, and Optimization of Coal Gasification-Based Energy and Chemical Processes", dx.doi.org/10.1021/ie3015654 | Ind. Eng. Chem. Res. 2012, 51, 15763-15777.